PERFORMANCE OF 130 kW MPD THRUSTER WITH AN EXTERNAL MAGNETIC FIELD AND LI AS A PROPELLANT

V.B. Tikhonov*
Research Institute of Applied Mechanics and Electrodynamics
of Moscow Aviation Institute, Moscow, Russia

S.A. Semenikhin**
Moscow Aviation Institute, Moscow, Russia

J.R. Brophy***, J.E. Polk****
Jet Propulsion Laboratory,
California, Institute of Technology., USA

ABSTRACT

A model of 100 kW lithium-fed MPD thruster was developed and its characteristics were studied at a power of up to 130 kW during a three-year work under the contract NASW-4851 between NASA and research institute of Applied Mechanics and Electrodynamics of Moscow Aviation Institute (RIAME MAI).

The design diagram of the thruster, procedure for calculating the characteristics and comparison of calculated values and test data are presented in this paper. Calculation dependencies are based on the physical model of the plasma acceleration processes improved on the basis of the results of magnetic-probe measurements of magnetic fields and currents in the thruster which allowed to define the Hall component for the thrust.

The ways for increasing the thruster specific impulse and thrust efficiency are outlined on the basis of theoretical and experimental studies.

INTRODUCTION

For the wide range of future space programs, demanding high-powered Electric Propulsion Thrusters (EPT), one of the most suitable thrusters is lithium fed MPD thruster with externally generated or self-induced magnetic field. The experimental studies of the lithium MPD thrusters' performances were held in Russia and, in particular, in MAI during the last 30 years. These studies show the applicability of such thrusters to the lunar and marsian space programs.

The assessments of the thruster parameters demonstrate the advantage of thrusters with externally generated magnetic field at the power level of 250-300 kW, specific impulse of 45-50 km/s and thrust efficiency 0.45-0.55. At the power from 300 kW up to over 1 MW per one module the applied field, generated by the solenoid is not a necessity.

The 100-150 kW lithium thruster was modelled and tested in MAI with JPL participation. The performance of this model of thruster is presented in this article.

THE EXPERIMENTAL MODEL OF THE THRUSTER AND PARTICULARITIES OF ITS DESIGN

The thruster design is presented in Fig. 1. The main elements of the thruster are: cathode unit, anode unit, solenoid, insulator between cathode and anode and the insulator between cathode heater and cathode case.

Cathode unit is composed of outer cathode case, which, in turn, contains a bundle of tungsten rods a 3 mm in diameter, tightly enclosed in the outlet part of the case.

This bundle represents a multichannel hollow cathode. The channel between outer and inner cathode cases with the spiral grooves (screw-thread) serves as a vaporizer of liquid lithium, supplying the cathode. Inside the cathode a graphite heater is installed. It heats the outer surface of the multichannel hollow cathode up to over 1300 K before the start up of thruster. This cathode preheating enables smooth and reliable thruster start up when the lithium supplies to cathode and voltage of 40 V is applied.

Insulators are made of boron aluminium nitride and are placed in the low temperature area..

The anode unit consists of contoured tungsten outlet and molibdenic sleeve, joined by welding.

---

* Doctor of Technical Sciences, professor, RIAME MAI

** Doctor of Technical Sciences, Research Engineer , MAI

*** Supervisor, Electric Propulsion and Plasma Technology Group, Member AIAA.

**** Technical Group Leader, Advanced propulsion Technology Group, Member AIAA.

Internal contour of the anode outlet complies with the direction of vector of the externally-generated magnetic field. The outlet anode diameter D_a = =160 mm, cathode diameter D_c=45 mm. Relation D_a/D_c = =3.55.

Solenoid serves for generation of the external magnetic field and provides magnetic induction value of 0.13 T when the current through the solenoid coils doesn't exceed 300 A. Current-carrying coils are made of water-cooled copper pipe with diameter d=10×1 mm.

Current is supplied to anode and cathode units through Molibdenic studs and flanges, which also serve as load-bearing elements, attaching the thruster to thrustmeasuring device.

PARTICULARITIES OF PLASMA ACCELRATION PROCESS AND CALCULATION OF THRUSTER PERFORMANCE.

In the 70-90 the experimental researches of electron density, electron temperature and potential distributions were conducted in accelerated plasma with probe methods involved. These researches as well as magneto-probe measurements of magnetic field and current distribution were carried out on a number of MPD thruster models of various power and design and enabled to determine main particularities of acceleration process.

In MPD thruster with self-induced and applied magnetic fields is mobility of stream boundary (the stream contains the majority of working agent mass). It is caused by joint action of pinch and Hall effects in plasma near the anode.

In the gap between electrods of applied-field MPD thruster there are three specific areas of plasma acceleration and relatively thin anode layer.

First area of gas-dynamic plasma acceleration is located near the symmetry axis of thruster (Fig. 2). In this area ion velocity is parallel to the longitudinal axis of thruster, Hall's parameter $\omega_e\tau_e << 1$.

In the 2nd area plasma acceleration is caused both by pressure gradient and by pressure of volumetric electromagnetic forces.Boundaries of the 2nd area are determined by the outer (external) boundary of the 1st area and by the line of magnetic force, passing through the outer diameter of cathode.

In this area lines of electric current are almost parallel to the lines of magnetic force of applied magnetic field. Plasma density is high enough and Hall's parameter is also less than unity.

Specific particularity of the 3-rd area is an almost constant distribution of radial components of the current density along the length of electrode system. This area is located between the lines of magnetic force, which pass through the outlet cathode diameter and anode outlet edge. As the results of probe and magneto-probe measurements show, an average value of Hall's parameter is: $\omega_e\tau_e \sim$ 2-3 [1], [2], [3].

In this area electromagnetic plasma acceleration occurs.

The results of current density measurements brought out the necessity of anode contouring along the lines of magnetic force, which provides more uniform current distribution and therefore the temperature of the anode surface.

The fourth specific area is the anode layer, which determines the conditions of charge transfer to the anode surface by plasma elements.

Dimension of this layer corresponds to the Larmor radius of electrons when measured normally to the anode surface.

The simplified parameter of charge transfer conditions in the anode layer and the influence of various factors on the variation of anode drop of voltage and electron current density is presented in [4].

Analysis of the conducted researches allowed to clarify the physical model of plasma acceleration processes and to define methods of calculation of MPD thruster integral characteristics.

CALCULATION OF THRUSTER CHARACTERISTICS.

Since thruster characteristics reflect integral dependencies of one of the parameters on the set of all the others, integral dependencies for thrust, specific impulse, power and thrust efficiency can serve as a base for characteristics calculation.

All these dependencies are known, but for their correct use it is necessary to determine calculated dependence for the thrust of MPD thruster, which corresponds well to results of the experiments.

In applied-field MPD thrusters 2 main mechanisms of acceleration are involved: gas-dynamic and electromagnetic. The thrust of MPD thruster has 3 components: gasdynamic, Hall's and electromagnetic (due to interaction of current with self-induced magnetic field):

$$T = T_{GD} + T_H + T_I \qquad (1)$$

Calculated dependencies for thrust components were presented in [8].

However, authors supposed it's possible to present these dependencies for readers' convenience.

$$T_{GD} = 1.6 \cdot a \cdot m \qquad (2)$$

$$T_H = 0.1 \cdot I \cdot B_A \cdot D_A \qquad (3)$$

$$T_I = 1.6 \cdot 10^{-7} \cdot I^2 \qquad (4)$$

Where a - sonic velocity at the multichannel cathode outlet ($a \sim 8.3 \cdot 10^3$ m/s; $T_e \sim$ 1.5 eV);I - discharge current; B_A -magnetic field at the anode outlet; D_A - outlet diameter of the anode.

Decreasing of thrust coefficient down to as low as 0.1 in comparison with calculated value [5] when electrode system geometry and magnetic fields are kept fixed is caused by increasing of current outflow length in the thruster. It occurs when the externally generated magnetic field of relatively small value is applied [6].

Current-voltage characteristics calculation appears to be more complex. Since method of current-voltage characteristics calculation wasn't presented in details earlier, we supposed to present it in more details in this paper.

As we know the calculated dependencies for thrust, we can calculate current-voltage and other characteristics of thruster using the integral balance of energy expenditures.

Power consumed by the thruster is determined as the sum of losses for the energy transfer processes in thruster and of electrodes' losses by radiation from plasma and of other losses.

$$N = U \cdot I = \sum_{i=1}^{n} N_i \qquad (5)$$

Hence potential difference on the electrodes can be presented as a sum of volt equivalent of expenditures.

$$U = \sum_{i=1}^{n} \Delta U_i \qquad (6)$$

$\Delta U_i = N_i / I$ - volt equivalent of particular expenditures.

Volt equivalent of expenditures for plasma acceleration is:

$$\Delta U_{acc} = T^2 / (2 \cdot \dot{m} \, I) \qquad (7)$$

Energy expenditures for the variation of working agent enthalpy are:

$$\Delta U_{enth.} = \frac{\beta_i \cdot e(U_i + \frac{2kT_e}{e}) N_A \, \dot{m}}{\mu_{pl} I} \qquad (8)$$

where

β_i - ionization coefficient
(for lithium $\beta_i = 1$);
U_i - ionization potential;
N_A - Avogadro number;
μ_{pl} - molecular weight of lithium plasma
($\mu_{pl} = 3.5$).

Energy losses in cathode have a value of 1-3 V in a wide range of discharge currents and are relatively low in comparison with the other losses.

$$\Delta U_C = 1\text{-}3 \ V \qquad (9)$$

Energy losses in thruster's anode are:

$$\Delta U_A = \varphi_A + \frac{2kT_e}{c} + \Delta U_A \qquad (10)$$

where

φ_A - work function of anode material;
T_e - temperature of electrons in the anode layer;
ΔU_A - anode drop of voltage.

Temperature of electrons in the anodic layer is higher then an average value in the volume and is as high as ~ 3 eV when working in the subcritical mode.

Value of anode-drop voltage depends on magnetic field, discharge current, and mass flow rate.

Experimental data processing shows that anode-drop voltage reaches its maximum value simultaneously with the appearance of the critical current regime and doesn't exceed 10 V.

It is determined by the binding energy of tungsten crystal lattice of 8.67 eV and by the ionization potential of tungsten atoms, which is 7.9 eV.

Taking these results into account, anode drop of potential can be determined from empirical dependence:

$$\Delta U_A = C \cdot 10^{-6} (I - I_0^2) + 45 B_c - 10^4 \cdot \dot{m} \qquad (11)$$

Critical current value is determined from the condition of ion-acoustic vibrations on the boundary of stability:

$$I_{cr.} B_C \cdot (R_A - R_C) \cdot 10^{-7} / (\mu \cdot \dot{m} \cdot a) =$$

$$= 3.6 / (R_A / R_C) - 0.5 \qquad (12)$$

where R_A, R_C - outlet edge radii of anode and cathode respectively;
$\mu = 4 \pi 10^{-7} \, H/m$; a - sonic velocity; B_C - magnetic field on the cathode outlet.

I_0 - value of discharge current, corresponding to anode drop voltage, which is less or equal to zero.

For 100-150 kWe thrusters with power of 100-150 kWe and mass flow rates of 70-100 mg/s, $I_0 = 10^3$ A can be assumed.

Having at values $I = I_{cr.}$; I_0 ; B_C ; $\dot{m}$, when $\Delta U_A = 10$ V, we can determine constant C and then find out the dependence of anode drop voltage on discharge current.

Determination of calculated value of voltage allows to find out the variation of thrust efficiency in various modes of operation.

Efficiency of plasma acceleration in thruster is:

$$\eta_{acc} = T^2 / (2 \, \dot{m} \, U \, I) = \Delta U_{acc} / U \qquad (13)$$

Full thrust efficiency, taking into account the losses by magnetic field and cathode heating will be:

$$\eta = T^2 / ((2\ m\ (U I + N_M + N_{CH})) \qquad (14)$$

Using the equations, presented above, calculations were conducted. They demonstrated that increasing of magnetic field for more than 0.1 Tl is inexpedient since it doesn't result in increasing of specific impulse and thrust efficiency of the thruster.

Main reason of it is decreasing of critical current due to increasing of magnetic field and losses growth.

Providing the conditions of thruster operation stability requires increasing of mass flow rate, which leads to conservation or decreasing of specific impulse value when limitation on discharge current exists.

EXPERIMENTAL MEASUREMENT OF CHARACTERISTICS.

Thrust, mass flow rate, discharge current, electrodes' voltage, power, consumed for cathode heating and for generation of external magnetic field (by solenoid) - all these parameters of the thruster were measured during the experiments.

Thrust characteristic is the linear function of current at various mass flow rates and magnetic fields.

Current-voltage characteristic deflects from the linear dependence when the current approximates its critical value because of anode drop voltage growth.

As it appeared to be, thrust efficiency increases with the power growth. Preliminary results of characteristics calculation for 100 kWe thruster are presented in [8].

Results of following experiments as well as their correspondence to calculated data are presented in Table 1 and in Fig. 3, 4, 5. These results confirm both the correctness of physical model of processes in the thruster and methods of characteristics calculation.

Possibility of the specific impulse and thrust efficiency increasing is associated with the extension of the range of stable operating modes, i. e. with critical current increasing.

Using the method of characteristics calculation, which is presented above, maximum possible parameters for lithium fed applied-field thrusters were determined.

Calculation results are presented in Table 2. They demonstrate it's possible to increase the specific impulse up to 50-55 km/s and thrust efficiency up to 50-55 % when the 200 kW thruster operates in nearly critical modes. But yet it requires adequate measures for enhancement of intensity of heat rejection from the anode outlet edge and, besides, strict control of the thruster operation mode in order not to exceed critical current level.

CONCLUSION

The model of lithium-fed 100 kW MPD thruster was developed and constructed. It demonstrated the stable operation at the power levels of up to 130 kW and the currents of 1700-2100 A, mass flow rates of 70-95 mg/s and magnetic field of 0.09 T.

Calculations of the thruster characteristics demonstrated that increasing of magnetic field for more than 0.1 Tl is inexpedient since it doesn't result in increasing of specific impulse and thrust efficiency.

Further modernization of the thruster will include decreasing of the anode diameter to cathode diameter ratio with keeping current density fixed at the level of 130-150 A/cm ^{2} of cathode cross-sectional area. This modernization will allow to increase the specific impulse up to 50 km/s and thrust efficiency up to 50-55 %.

Decreasing of intensity of erosion processes in multichannel cathodes remains to be one of the main problems of this type thrusters.

REFERENCES

1. A.G. Popov, G.Ja. Portnov, S.A. Semenikhin et al.
   "Experimental Investigation of Magetic Fields and Currents in Butt-HallThrusters". Collection of Papers "Ion Injectors and Plasma Acceletors". Moscow, Energoatomizdat, 1990, pp. 97-105.
2. V.V. Zhurin, A.G. Popov, V.B. Tikhonov et al.
   "The State of Research and Development of End-Hall Thrusters in the USSR".IEPC-91-080. Presented at the 22nd International Electric Propulsion Conference. October 14-17, 1991, Viarregio, Italy.
3. A.G. Popov, V.B. Tikhonov.
   "Theoretical and Experimental Research on Magnetoplasmadynamic Thrusters". Proceedings Paper RGC-EP-92-16, Presented at the 1st Russian-German Conference on Electric Propulsion and Their Technical Application. Giessen, Germany, March 9-14, 1992.
4. N.V. Belan, V. Kim, A.I. Oranski,V.B. Tikhonov.
   "Stationary Plasma Thrusters"Kharkov, Kharkov Aviation Institute, 1989 (in Russian)
5. A.G. Popov, S.A. Semenikhin
   "The Thrust Calculation for the EHT Thrusters". Proc. 7th Soviet Conference on Plasma Accelerators and Ion Injectors. Kharkov, 1989 (in Russian).
6. G.A. Diakonov, V.B. Tikhonov.
   "The Experimental Investigation of Acceleration Channel Geometry and Magnetic Field Influence of the Plasma Flow Regime in the Co-axial Quasi-

6. G.A. Diakonov, V.B. Tikhonov. "The Experimental Investigation of Acceleration Channel Geometry and Mag netic Field Influence of the Plasma Flow Regime in the Co-axial Quasi-stationary Plasma - 50 type Acceleration". Plasma Physics,1994, v.20, pp.553-540, Moscow (in Russian).
7. V.B. Tikhonov, S.A. Semenikhin et al. "Research of Plasma Acceleration Proc esses in Self-field and Applied Magnetic Field Thrusters".IEPC-93-076. Presen ted at the 23rd International Electric Propulsion Conference, Seattle,September 13-16, 1993.
8. V.B. Tikhonov, S.A. Semenikhin, J.R. Brophy, J.E. Polk. "The Experimental Performance of the 100 kW Li Thruster with External Magnetic Field". IEPC-95-105.Presented at the 24th International Electric Propulion Conference, Moscow, September 19-23, 1995.

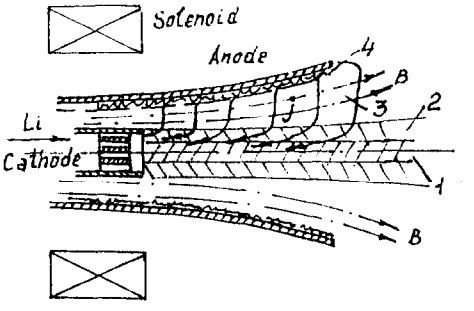

Fig 2. Caracteristic area in thruster

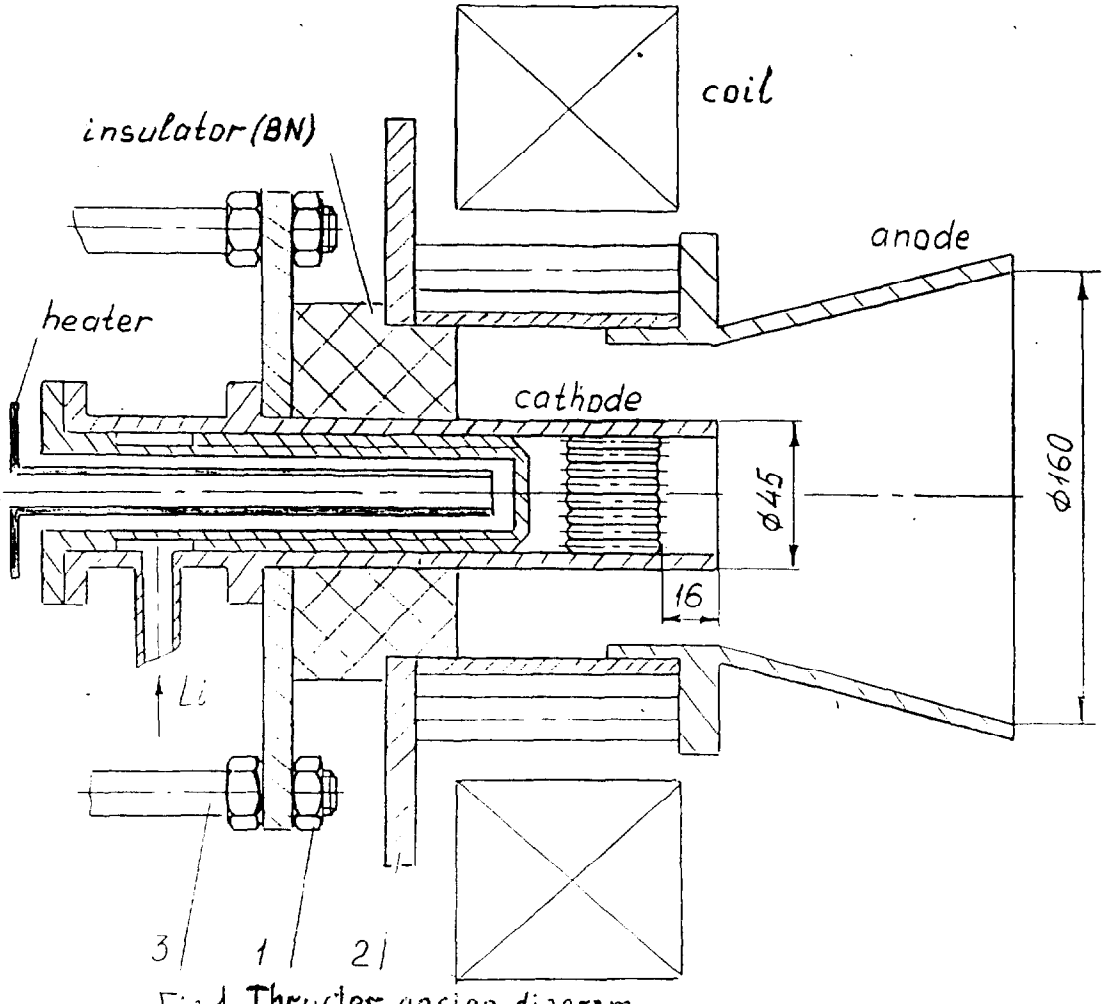

Fig 1 Thruster gesign diagram

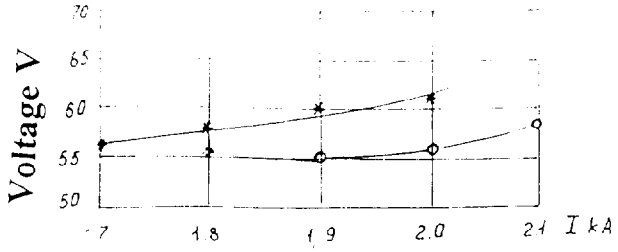

Fig. 3. Current-Voltage characteristics.

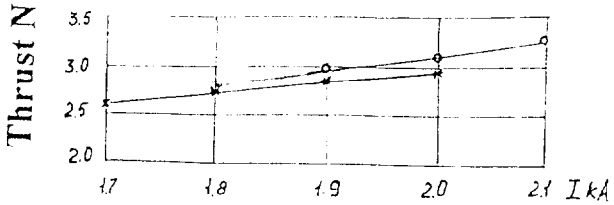

Fig. 4. Thrust characteristics.

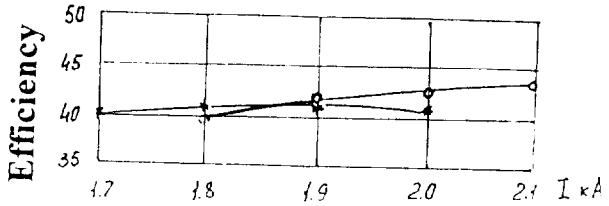

Fig. 5. Efficiency characteristics
B_c=0,09T *$\dot{m}$=81mg/s °$\dot{m}$=94mg/s

Table 2
B_c = 0.09 T

$\dot{m}$, mg/s	80		85		90	
D_A/Dc	3.0	3.2	3.0	3.2	3.0	3.2
I_{cr}, kA	3.43	2.88	3.64	3.06	3.86	3.24
T_Σ, N	4.61	3.88	5.01	4.21	5.46	4.55
I_{sp}, km/s	57.6	48.5	58.9	49.5	60.7	50.6
U, V	68	64	70	64	70	66
N_Σ, kW	243	194	265	206	288	224
η_Σ	0.55	0.49	0.56	0.51	0.58	0.54

Table 1.

Theory	B = 0.09 T	$\dot{m}$ = 80 mg/s			
Experim.	B = 0.09 T	$\dot{m}$ = 81 mg/s			
I, kA	T, N	$I_{sp.}$, km/s	U, V	$\eta_{e.}$	η_Σ
1.7	2.53 2.58	31.60 32.00	54.4 56.5	0.432 0.435	0.397 0.399
1.8	2.64 2.72	33.00 33.60	55.3 57.5	0.438 0.441	0.405 0.410
1.9	2.74 2.86	34.25 35.30	56.2 60.0	0.440 0.443	0.409 0.414
2.0	2.86 2.93	35.75 36.20	57.4 61.0	0.446 0.43	0.417 0.407
2.1	2.91	37.25	58.1	0.455	0.427
Theory	B = 0.09 T	$\dot{m}$ = 85 mg/s			
Experim.	B = 0.09 T	$\dot{m}$ = 86 mg/s			
I, kA	T, N	$I_{sp.}$, km/s	U, V	$\eta_{e.}$	η_Σ
1.7	2.61 2.70	30.60 31.40	54.4 55.0	0.432 0.453	0.398 0.416
1.8	2.72 2.80	32.00 32.60	55.1 57.0	0.439 0.445	0.406 0.420
1.9	2.82 -	33.20 -	55.8 -	0.441 -	0.411 -
2.0	2.94 -	34.40 -	56.6 -	0.447 -	0.421 -
2.1	3.06 -	36.00 -	57.3 -	0.457 -	0.430 -
Theory	B = 0.09 T	$\dot{m}$ = 95 mg/s			
Experim.	B = 0.09 T	$\dot{m}$ = 94 mg/s			
I, kA	T, N	$I_{sp.}$, km/s	U, V	$\eta_{e.}$	η_Σ
1.7	2.70 -	30.00 -	54.2 -	0.439 -	0.405 -
1.8	2.80 2.84	31.10 29.90	54.5 56.0	0.444 0.421	0.410 0.390
1.9	2.90 2.98	30.90 31.70	54.9 55.0	0.424 0.452	0.400 0.418
2.0	3.02 3.15	33.60 33.5	55.9 56.0	0.454 0.471	0.423 0.439
2.1	3.14 3.29	34.60 35.00	56.6 58.0	0.458 0.472	0.428 0.442